

**Parametrically forced surface wave with a nonmonotonic dispersion relation**

Hee-kyoung Ko and Kyoung J. Lee\*

*National Creative Research Initiative Center for Neuro-dynamics and Department of Physics, Korea University, Seoul 136-701, Korea*

Jysoo Lee

*Supercomputing Center, Korea Institute of Science and Technology Information, Yusong-Gu, Eoeun-Dong 52, Daejeon 305-806, Korea*

(Received 25 November 2002; published 26 February 2003)

Surface wave patterns that arise in a *mechanically* driven ferrofluid system under constant magnetic field are investigated (1) to find out what kind of spatial patterns emerge when the system acquires a nonmonotonic dispersion relation and (2) to compare its surface wave patterns with those produced in the *magnetically* driven system studied earlier. As the strength of the applied magnetic field increases, the initial subharmonic square lattice formed by the Faraday instability first transforms to rolls, then becomes a rhomboid lattice. The rolls and the rhomboid lattice are found to coexist for a finite range of parameter space forming patterns with mixed domains. Possible underlying mechanisms for the observed rhomboid lattice is discussed. None of the diverse superlattices observed in the magnetically driven ferrofluid system appears in the mechanically driven system studied here.

DOI: 10.1103/PhysRevE.67.026218

PACS number(s): 05.45.-a, 47.54.+r, 05.65.+b, 89.75.-k

**I. INTRODUCTION**

Nonequilibrium patterns arising in spatially extended systems have been a subject of great scientific interest over the past years, and one of its new challenges is to understand the systems having several unstable modes simultaneously [1–14]. In such a system, there can be situations in which the final steady state consists of a number of domains with different wave numbers being separated by domain walls. This possibility was shown earlier by Raitt and Riecke in a model study based on a set of Ginzburg-Landau equations [1,2] and, subsequently, was proven by Mahr and Rehberg in an experiment, using a Faraday system employing ferrofluid [3,4]. The model system exhibited stable patterns with multiple domains having different wave vectors due to its nonmonotonic dispersion relation (i.e., its neutral curve has multiple minima), and the surface waves in the ferrofluid system studied by Mahr and Rehberg were actual examples exhibiting such a nonmonotonic dispersion relation. Both studies were, however, limited to one dimension in space.

A quite interesting situation may arise when such a system is extended to two-dimensional space: instead of patterns with multiple domains, a variety of complex superlattices and quasicrystalline patterns can be produced by so-called “resonant mode interactions” among the unstable modes [6,8–12,14]. The first experimental system addressing this phenomenon was “two-frequency forced Faraday system” in which two different spatial modes were forced to emerge by various combinations of two sinusoidal forcings [6,8]. Here, the use of two-frequency driving was to excite two different spatiotemporal modes simultaneously bringing the system to a bicritical situation. Various intriguing superlattices and quasicrystal patterns were observed in such systems. Recently, however, it was demonstrated that similar

superlattice patterns can also be realized even in a single frequency forced Faraday system, that is, a magnetically driven ferrofluid system [10,11]. Various superlattices (in addition to the squares, hexagons, and rhombus) were revealed in this system as well.

The underlying mechanisms of these ferrofluid superlattice patterns, however, were not so evident. Although some of them were shown to arise due to a bicriticality formed by the harmonic hexagonal mode related to the Rosensweig instability and the subharmonic square mode of the Faraday instability, many of the observed superlattices could not be explained by a simple three-wave interaction between the two basic modes [11]. They might have arisen through higher-order resonant mode interactions. Yet, this is quite difficult to prove or disprove. Incidentally, these patterns might have emerged with a quite different mechanism: as discussed before, the surface waves in a driven ferrofluid can exhibit a nonmonotonic dispersion relation under a suitable condition; thus, multiple Fourier modes can be excited simultaneously even without the bicriticality. In this viewpoint, one major complication in understanding the complex patterns observed in the magnetically driven ferrofluid system is the fact that the dispersion relation changes as the applied magnetic field oscillates in time.

Here, we have examined two-dimensional surface wave patterns that arise in a *mechanically* driven dish containing ferrofluid under a constant magnetic field. Since we are now employing a mechanical forcing scheme (instead of the magnetic forcing), the complication of the oscillating dispersion relation no longer exists. More explicitly, we are interested in knowing what would happen to the surface wave pattern as its dispersion relation becomes nonmonotonic, in particular, in two-dimensional space. Thus, our current system can be also viewed as a two-dimensional extension of the one-dimensional system studied earlier by Mahr and Rehberg [4].

Surprisingly, in the mechanically driven ferrofluid system only simple patterns such as squares, rolls, and rhombus are observed. All those complex superlattice patterns observed in

---

\*Author to whom correspondence should be addressed. Email address: kyoung@nld.korea.ac.kr

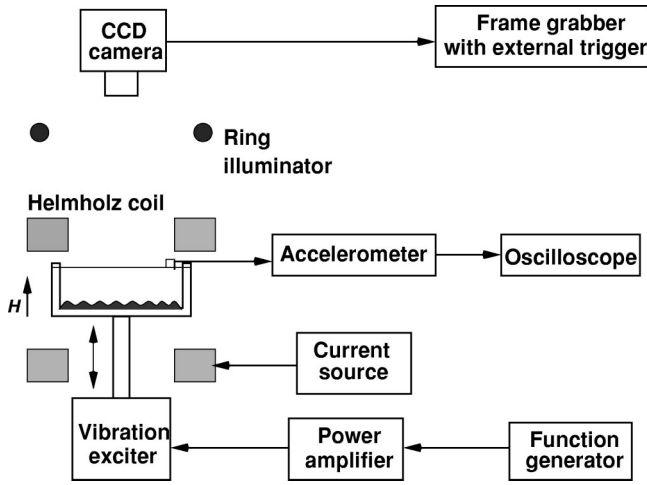


FIG. 1. Mechanically driven ferrofluid system under a constant magnetic field.

the magnetically forced ferrofluid system are no longer seen. The existence of the rhomboid pattern is, nevertheless, quite significant for its two distinct wave vectors. It is also found that the rhomboid pattern can also coexist with the roll pattern for some finite range of the control parameter. Possible underlying mechanisms of the rhomboid pattern are discussed with a set of two-dimensional amplitude equations extended from the one-dimensional model developed earlier by Raitt and Riecke [2].

## II. EXPERIMENTAL SETUP

Our experimental setup is schematically depicted in Fig. 1. It is composed of a teflon container containing ferrofluid, a mechanical vibrator, a pair of Helmholtz coils, and an imaging system. The cylindrical teflon container has a physical dimension of depth 50 mm and inner diameter 140 mm and has an air-tight glass cover. The ferrofluid that we used is a one-to-one mixture of two commercially available ones (EMG901 and EMG909, Ferrofluidics) [15,16]. The base of the ferrofluid container (fluid depth 1.0 mm) is firmly attached to a mechanical vibrator (PM vibration exciter 4808, Brüel & Kjær) and the assembly is placed in the middle of a pair of two Helmholtz coils according to the schematic diagram in Fig. 1. Sinusoidal signals are generated by a function generator, amplified by a linear amplifier (power amplifier 2712, Brüel & Kjær), then fed to the mechanical vibrator to drive the container. The vertical acceleration of the container is monitored by a charge accelerometer (model 4393, Brüel & Kjær) attached to the glass cover. The Helmholtz coils have an inner (outer) diameter of 200 (280) mm, and the separation between them is 120 mm. The stability of the magnetic field is monitored with a hall probe (Model 6010, F. W. Bell Inc.) to confirm its spatial variation is within 3% in the interested area.

The fluid surface is illuminated by three concentric light-emitting diode array rings (homebuilt diameter 160, 180, and 200 mm, respectively) for uniform illumination. They are placed about 275 mm above the surface of ferrofluid. The patterns are imaged at a spatial resolution of  $530 \times 512$  pixels

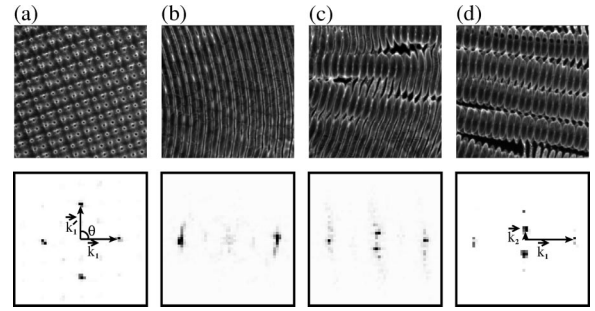


FIG. 2. Standing wave patterns and their Fourier transform images acquired in a driven ferrofluid system: (a) squares,  $H=0$ ; (b) rolls,  $H=0.88H_c$ ; (c) mixed state of rolls and rhomboid pattern,  $H=0.90H_c$ ; and (d) rhomboid pattern,  $H=0.94H_c$ . Here,  $H_c = 100.7$  G is the critical field of the static Rosensweig instability for the ferrofluid being used. The system is driven at  $f=70$  Hz with an acceleration  $\Gamma=22.8$  m/s<sup>2</sup> unless otherwise mentioned. Each frame is  $31 \times 31$  mm<sup>2</sup>.

by using a charge-coupled device camera (Quantix, Phothometrics) with a frame grabber (Meteor2/DIG, Metrox). The exposure time is set to be 3 ms. The camera is located at 560 mm above the fluid surface. The flat surfaces either above or below the level of surrounding fluid appear white, while the nonflat surface that scatters the light away from the camera appears black.

## III. EXPERIMENTAL RESULT

A wide range of parameter space is explored only to find simple lattices such as the subharmonic squares, rolls, rhombus, and mixed states (of rolls and rhombus), as shown in Fig. 2. Temporally subharmonic standing wave in the form of square lattice [see Fig. 2(a)] arises through the well-known Faraday instability in the absence of magnetic field. The two pairs of Fourier peaks crossing each other in a right angle are quite clear in the accompanying Fourier transform image.

The square lattice becomes unstable as the strength of the applied magnetic field increases. First, it transforms to a roll pattern [see Fig. 2(b)], as one pair of the Fourier peaks decays and disappears. The transition to the roll pattern takes place rather abruptly near  $H=0.88H_c$ , as shown in Fig. 3(a). The order parameter  $\alpha$  is the ratio  $P(\vec{k}'_1)/P(\vec{k}_1)$ , where  $P(\vec{k}_1)$  and  $P(\vec{k}'_1)$  are the spectral powers belonging to  $\vec{k}_1$  and  $\vec{k}'_1$  modes, respectively. Toward this transition, the fluctuation of angle  $\theta$  between two base wave vectors  $\vec{k}_1$  and  $\vec{k}'_1$  increases significantly, although its mean value stays more or less near  $90^\circ$  [see Fig. 3(b)]. The increasing angular fluctuation is due to the emergence of domains and defect lines.

When the strength of the applied field is further increased from the roll pattern, a long wavelength modulation kicks into the system—first, locally and randomly [see Fig. 2(c)], and eventually in a more organized fashion producing the rhomboid pattern of Fig. 2(d). The corresponding Fourier transform images exhibit two pairs of wave vectors ( $\vec{k}_1$  and  $\vec{k}_2$ ) that are quite different in size [see Fig. 4(a)].

The transition from the roll pattern to the rhomboid pat-

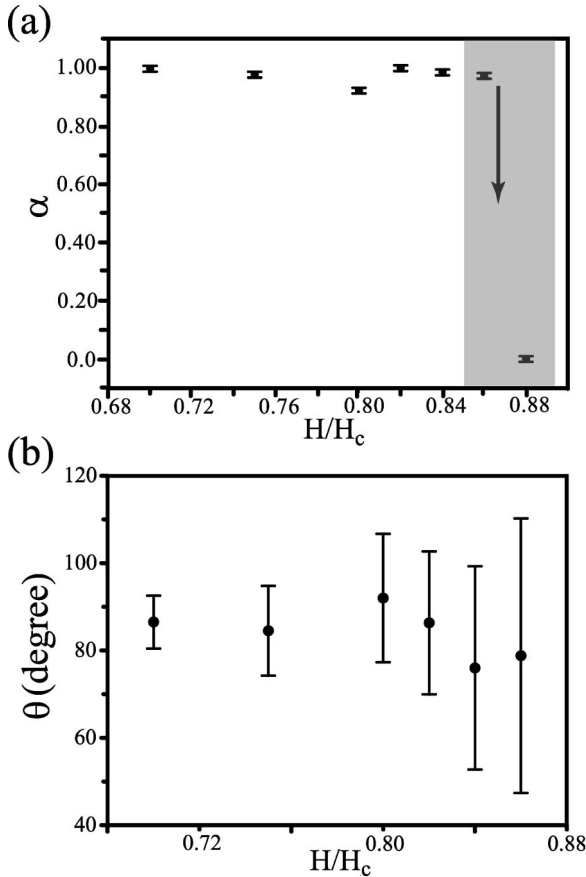


FIG. 3. Transition of square lattice to roll pattern: (a)  $\alpha = P(\vec{k}'_1)/P(\vec{k}_1)$  vs  $H$  and (b)  $\theta$  vs  $H$ ;  $\theta$  is measured in the real space.

tern is quantified in Fig. 4(b) by the order parameter  $\beta = P(k_2)/P(k_1)$ , where  $P(k_1)$  and  $P(k_2)$  are the spectral powers belonging to  $k_1$  and  $k_2$  modes, respectively. According to Fig. 4(b), the transition to the rhomboid pattern seems continuous. But this interpretation may be misleading since the roll pattern does coexist with the rhomboid pattern in a significant range of parameter space [i.e., within the shaded area in Fig. 4(a)]. In other words, the domains of rhomboid lattice grow gradually at the expense of shrinking domains of rolls; thus it is quite difficult to pinpoint the onset of the transition. The values of two wave vectors  $k_1$  and  $k_2$  do not change significantly over the whole parameter range of  $H$  that we have studied and seem not to be related to each other [see Fig. 4(a)] (i.e.,  $k_2$  is definitely not a subharmonic mode of  $k_1$ ).

Experimental investigation has also been carried out for other sets of driving frequency  $f$  and acceleration  $\Gamma$  only to find a similar sequence of transitions. For the wide range of parameter space that we have explored, the four classes of states presented in Fig. 2 are all that we have observed.

#### IV. MODEL AMPLITUDE EQUATION

In the limit of no viscosity and infinite depth, the dispersion relation for the plane wave of wave number  $k$  on the surface of a ferrofluid is

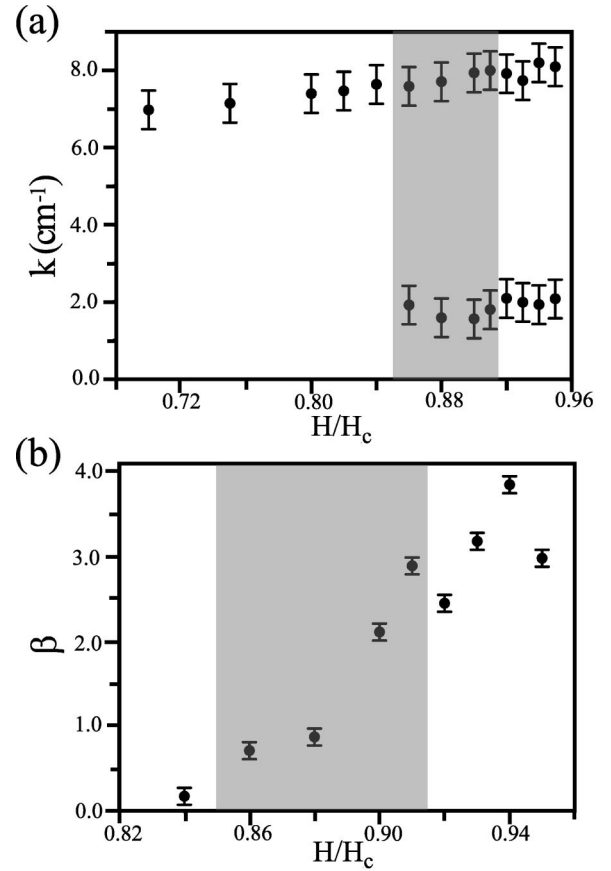


FIG. 4. Transition of rolls to rhombus: (a)  $k_1$  and  $k_2$  vs  $H$  and (b)  $\beta = P(k_2)/P(k_1)$  vs  $H$ . The values of  $k_1$  and  $k_2$  are obtained by identifying two local maximum peaks along the radial function, that is, obtained by azimuthally averaging the Fourier image.  $P(k_1)$  and  $P(k_2)$  are the average spectral powers belonging to  $k_1$  and  $k_2$ , respectively. The rolls coexist with the rhomboid pattern for the shaded area.

$$\omega^2(k) = gk + \frac{\sigma}{\rho}k^3 - \frac{1}{\rho(1/\mu_o + 1/\mu)}M_o^2k^2, \quad (1)$$

where  $g$  is the gravitational acceleration,  $\sigma$  is the surface tension,  $\rho$  is the density of the fluid,  $\mu$  is the permeability, and  $M_o$  is the magnetization of the fluid [15]. For  $M_o^2 > M_c^2 = \sqrt{3}g\sigma\rho(1/\mu_o + 1/\mu)$ , the dispersion relation becomes non-monotonic.

In recent years, Raitt and Riecke [2] have developed an amplitude equation suitable for systems having a non-monotonic dispersion relation. They have proposed the following one-dimensional model equations:

$$\begin{aligned} \partial_t A + v \partial_x A &= d \partial_x^2 A + f \partial_x^3 A + aA + bB^* - c|A|^2 A - c'|B|^2 A, \\ \partial_t B - v \partial_x B &= d \partial_x^2 B - f \partial_x^3 B + aB + bA^* - c|B|^2 B - c'|A|^2 B. \end{aligned} \quad (2)$$

Here,  $A(x,t)$  [ $B(x,t)$ ] is the amplitude of the right (left) traveling plane wave. All the coefficients are complex except  $b$ , which is related to the magnitude of the parametric driving. The most significant change from the conventional am-

plitude equations is that second- and third-order spatial derivative terms are newly adopted. Raitt and Riecke argue that these two terms should be kept as long as  $\omega(k)$  has quadratic and cubic terms.

Linear stability analysis of the one-dimensional standing wave arising in the model system is carried out, and the neutral stability curve is found to be a nonmonotonic function:

$$b^2 = |a - ivk - dk^2 - ifk^3|^2. \quad (3)$$

Direct numerical simulation studies of Eq. (2) also have confirmed that multiple (two or three) bands of  $k$  can be simultaneously unstable. In other words, the existence of a nonmonotonic  $\omega(k)$  enables standing waves with multiple wave numbers.

In order to gain some insight into the observed patterns and their transitions in the experiment, we have extended Eq. (2) for the two-dimensional space, according to the standard procedure given in [17]. The extended set of equations is

$$\begin{aligned} \partial_t A + v \left( \partial_x - \frac{i}{2k_o} \partial_y^2 \right) A &= d \left( \partial_x - \frac{i}{2k_o} \partial_y^2 \right)^2 A \\ &+ f \left( \partial_x - \frac{i}{2k_o} \partial_y^2 \right)^3 A + aA + bB^* \\ &- c|A|^2 A - c'|B|^2 A, \\ \partial_t B + v \left( -\partial_x - \frac{i}{2k_o} \partial_y^2 \right) B &= d \left( -\partial_x - \frac{i}{2k_o} \partial_y^2 \right)^2 B \\ &+ f \left( -\partial_x - \frac{i}{2k_o} \partial_y^2 \right)^3 B + aB \\ &+ bA^* - c|B|^2 B - c'|A|^2 B, \end{aligned} \quad (4)$$

where  $k_o$  is the wave number associated with the primary instability. With a linear stability analysis, we find the following neutral stability *surface*:

$$b^2 = |a - ivk_+ - dk_+^2 - ifk_+^3|^2, \quad (5)$$

where  $k_+ = k_x + k_y^2/(2k_o)$ . This equation is basically the same as the neutral stability curve in one dimension [Eq. (3)] except that  $k$  is replaced by  $k_+$ .

A typical neutral stability surface is given in Fig. 5. The two unstable bands of the one-dimensional curve [Eq. (3)] are now replaced by two nearly parallel “troughs.” In this particular example, as one increases  $b$  the first modes to be excited are those in the band around  $k_x \sim 0.4$  ( $b \sim 0.53$ ). The second band locates around  $k_x \sim -0.8$  with  $b \sim 0.71$ . We note that along both troughs the minimum values of  $b$  do not change significantly. This suggests that a wide range of  $k_y$  modes can be present in the final pattern. In other words, one may expect that the orientation of the standing wave (as determined by the ratio of  $k_y$  to  $k_o + k_x$ ) can be varied without changing its stability significantly.

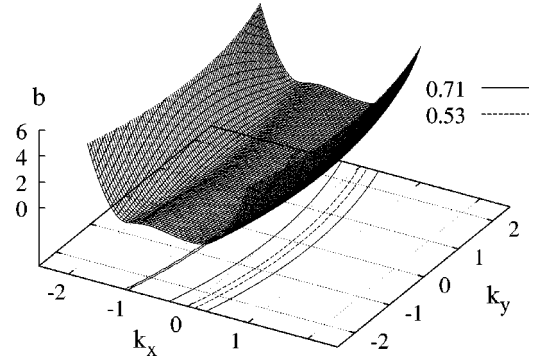


FIG. 5. Neutral stability surface of Eq. (4) with  $a = -0.5 + 0.5i, d = 0.1, v = 1 + 0.2i, f = -3$ . Two parallel “troughs” of instability bands are observed.

In fact, in the experiment we observe that the regular roll pattern [Fig. 2(b)] becomes progressively less regular [Fig. 2(c)] until it stabilizes to a rhomboid state [Fig. 2(d)], as the parameter  $H$  increases. From this viewpoint, the rhomboid lattice of Fig. 2(d) can be considered as “deformed rolls.” This interpretation is similar to that provided by Ouyang *et al.* for that the rhomboid lattice in their study is viewed as a deformed hexagonal lattice [18].

The same neutral stability surface can, however, suggest a different mechanism for the rhomboid lattice of Fig. 2(d)—unstable  $k$  modes from different stability bands are excited at the same time but in different directions. We note that the wave number in one direction (along  $k_x$  axis) is significantly larger than that in the other direction (along  $k_y$  axis), and it is possible that each mode belongs to a different stability band. Experimental verification of the exact underlying mechanism of the rhomboid pattern would, however, require a better spatial resolution in the Fourier space. Our current experimental system is not large enough to accommodate a large number of  $k_2$  modes.

## V. CONCLUSION

We have shown that under a suitable condition the surface wave of a ferrofluid can have a nonmonotonic dispersion relation producing two unstable modes simultaneously. Two-dimensional patterns with coexisting domains of different wave numbers are observed, as in the relevant one-dimensional studies conducted earlier [2,4]. So far, the paper by Residori *et al.* [5] is the only other experimental study that has demonstrated the existence of coexisting domains (there, in particular, hexagons and stripes) in two-dimensional space. Unfortunately, however, the precise origin of the domain patterns is not yet established. Indeed, no one has yet to discuss rigorously what are the possible two-dimensional domain structures for a system with two or more spatial modes gone unstable simultaneously.

On the other hand, there is no reason why not the same two-dimensional system produces regular lattice patterns, instead of domains. With two distinct unstable wave numbers  $k_1$  and  $k_2$  present, one can naturally expect either a zigzag state [1,19] or a rhomboid pattern [7] to arise. Theoretically, the stability of zigzag structure has been studied in some

detail, but very little for rhomboid pattern.

It is also important to note that none of the diverse superlattice patterns observed earlier in the magnetically driven ferrofluid system [11] does not appear in the current system employing a mechanical forcing scheme. In other words, the two independent Fourier modes generated by the nonmonotonic dispersion do not produce any resonant modes. Subsequently, we can speculate that all those resonant superlattice patterns observed in the magnetically forced system had arisen by some resonant interactions between the harmonic hexagon of the Rosensweig instability and the subharmonic square of the Faraday instability and had not originated from the nonlinear dispersion property of the magnetic fluid. It is, however, still uncertain what had the oscillating dispersion relation caused to the patterns in the magnetically driven system.

Finally, we also like to indicate that the issues we discuss here can be extended to traveling waves. Theoretically, very little is known about domain structures of traveling waves and they are of great scientific interest currently. Incidentally, a recent experimental study on excitable waves in a Belousov-Zhabotinsky reaction-diffusion system reports interesting traveling wave states with bunching wave fronts [20]. They also originate from a nonlinear dispersion relation.

#### ACKNOWLEDGMENT

This work was supported by Creative Research Initiatives of the Korean Ministry of Science and Technology.

- 
- [1] D. Raitt and H. Riecke, *Physica D* **82**, 79 (1995).
  - [2] D. Raitt and H. Riecke, *Phys. Rev. E* **55**, 5448 (1997).
  - [3] T. Mahr, A. Groisman, and I. Rehberg, *J. Magn. Magn. Mater.* **159**, L45 (1996).
  - [4] T. Mahr and I. Rehberg, *Phys. Rev. Lett.* **81**, 89 (1998).
  - [5] S. Residori, P.L. Ramazza, E. Pampaloni, S. Boccaletti, and F.T. Arecchi, *Phys. Rev. Lett.* **76**, 1063 (2001).
  - [6] W.S. Edwards and S. Fauve, *J. Fluid Mech.* **278**, 123 (1994).
  - [7] R. Lifshitz and D.M. Petrich, *Phys. Rev. Lett.* **79**, 1261 (1997).
  - [8] A. Kudrolli, B. Pier, and J.P. Gollub, *Physica D* **123**, 99 (1998).
  - [9] H. Arbell and J. Fineberg, *Phys. Rev. E* **65**, 036224 (2001).
  - [10] H.-J. Pi, S.-y. Park, J. Lee, and K.J. Lee, *Phys. Rev. Lett.* **84**, 5316 (2000).
  - [11] H.-k. Ko, J. Lee, and K.J. Lee, *Phys. Rev. E* **65**, 056222 (2002).
  - [12] C. Wagner, H.W. Müller, and K. Knorr, *Phys. Rev. E* **62**, R33 (2000).
  - [13] M. Silber and A.C. Skeldon, *Phys. Rev. E* **59**, 5446 (1999).
  - [14] D.P. Tse, A.M. Rucklidge, R.B. Hoyle, and M. Silber, *Physica D* **146**, 367 (2000).
  - [15] R.E. Rosensweig, *Ferrohydrodynamic* (Cambridge University Press, Cambridge, 1993).
  - [16] The physical properties of EMG901 (EMG909) ferrofluids are the following: density  $\rho=1.53$  (1.02) g/ml, surface tension  $\sigma=27.5$  g/s<sup>2</sup>, initial magnetic susceptibility  $\chi=3.00$  (0.80), magnetic saturation  $M_s=600$  (200) G, dynamics viscosity  $\eta=10$  (6) cP, yielding a critical field of static Rosensweig instability at  $H=90.5$  (168.2) G, respectively.
  - [17] See, e.g., M. Cross and P. Hohenberg, *Rev. Mod. Phys.* **65**, 851 (1993).
  - [18] Ouyang, *et al.*, *Chaos* **3**, 707 (1993).
  - [19] B. Malomed, A. Nepomnyashchy, and M. Tribelsky, *Phys. Rev. A* **42**, 7244 (1990).
  - [20] C.T. Hamik and O. Steinbock, *Phys. Rev. E* **65**, 046224 (2002).